Polymer 50 (2009) 3285–3291

Contents lists available at ScienceDirect

Polymer

journal homepage: www.elsevier.com/locate/polymer

Preparation of polystyrene–multiwalled carbon nanotube composites with individual-dispersed nanotubes and strong interfacial adhesion

Jian-Min Yuan [a,*], Ze-Fu Fan [a], Xiao-Hua Chen [a,*], Xian-Hong Chen [a], Zhen-Jun Wu [b], Li-Ping He [c]

[a] College of Material Science and Engineering, Hunan University, South Road of Yuelu Zone, Changsha 410082, PR China
[b] College of Chemistry and Chemical Engineering, Hunan University, Changsha 410082, PR China
[c] College of Mechanical and Automobile Engineering, Hunan University, Changsha 410082, PR China

ARTICLE INFO

Article history:
Received 18 November 2008
Received in revised form
24 April 2009
Accepted 29 April 2009
Available online 8 May 2009

Keywords:
Multiwalled carbon nanotubes
Interfacial adhesion
Polystyrene

ABSTRACT

Multiwalled carbon nanotubes (MWCNTs) were modified via polymerization of styrene under microwave irradiation, and polystyrene (PS)–MWCNT composites with individual-dispersed nanotubes were prepared by melt-mixing using industrial extruder and injection moulding machine. The microscopic morphologies of modified MWCNTs (m-MWCNTs) and composites were studied through transmission electronic microscopy and scanning electron microscopy. Result showed that a PS coat layer was introduced on the m-MWCNT surfaces, improving the compatibility of nanotubes with poor polar materials such as tetrahydrofuran, toluene, and PS matrix. Contrary to the composite prepared directly using purified MWCNTs (PS–p-MWCNT composite) without further modification, the composite prepared using m-MWCNTs (PS–m-MWCNT composite) exhibited a PS middle layer between nanotubes and matrix, leading to a strong interfacial adhesion. Thereby, although the nanotubes are individually dispersed in both PS–p-MWCNT and PS–m-MWCNT composites, the mechanical property of the latter is better than that of the former. When the nanotube content is 0.32 wt%, the PS–m-MWCNT composite had a 250% increase of impact strength as compared to pure PS, but the PS–p-MWCNT composite had only a 150% increase. Furthermore, the tensile strength of PS–p-MWCNT composite descended slightly with the addition of nanotube content, whereas, that of the PS–m-MWCNT composite ascended slightly.

1. Introduction

Composites of carbon nanotubes (CNTs) in polymeric matrices have attracted considerable attention in the research and industrial fields due to their good electrical conductivity, high stiffness, and high strength at relatively low CNT contents [1–4]. It is widely recognized that the quality of composites strongly depends on the dispersion of CNTs in polymer matrices. In most of the cases homogeneous dispersion of nanotubes is hindered by both synthesis induced 'entangled' and 'aggregated' structures of nanotubes as well as the tubes' tendency to form agglomerates, due to the intermolecular van der Waals interactions. Currently, three most common methods are used to introduce CNTs into polymer: (1) solution-mixing [5,6], (2) in situ polymerization of CNTs–polymer monomer mixture [7,8], and (3) melt-mixing of CNTs with polymer melts [9,10].

A problem with solution-mixing is the evaporation of a large amount of solvent, which makes this method impractical for mass production. At the same time, for a chemically resistant polymer such as high-density polyethylene, only a few toxic solvents (for example, toluene and xylene) can partially dissolve it at high temperatures (e.g. 100 °C). In situ polymerization seems to be a promising method to fabricate polymer–CNT composites. However, before this method can be used in industrial scale processes, the difficult problem of dispersing CNTs uniformly into a large amount of solution still exists.

In melt-mixing, CNTs are mechanically dispersed into a polymer melt (prepared by heating) using a mixer or a compounder [10]. The central idea is to use fluid shear forces to break nanotube aggregates or prevent their formation [11]. This approach is simple and compatible with existing polymer processing techniques such as extrusion, injection moulding and compression moulding. Therefore it holds promise for use in large-scale industrial applications. Here, two ways for introducing nanotubes in polymer matrices by melt-mixing are used. In the first case, nanotubes are directly incorporated into the polymer matrix [12–14]. In the other case, commercially available masterbatches of polymer–nanotube composites [15] are used as the starting materials which are diluted

* Corresponding authors.
E-mail addresses: pangyuan2916@126.com (J.-M. Yuan), hudacxh62@yahoo.com.cn (X.-H. Chen).

0032-3861/$ – see front matter © 2009 Elsevier Ltd. All rights reserved.
doi:10.1016/j.polymer.2009.04.065

with the pure polymer in a subsequent melt-mixing process [16]. Haggenmueller et al. [17] showed an enhanced singlewalled (SW) CNT dispersion after melt-processing of polymethylmethacrylate (PMMA)–SWCNT composites which were prepared by solution-mixing. Jin et al. [18] used a miniature mixer-molder (ATLAS) to produce small quantities (approximately 0.4 g) of well-dispersed mixtures of multiwalled (MW) CNT in PMMA. Lozano and Barrera [19,20] used a haake miniature laboratory mixer (14–20 g) to disperse vapor grown carbon fibers in polypropylene. However, preparations on kilogram quantities of well-dispersed polymer–nanotube composites using industrial extruder and injection moulding machine [21–23] were rarely reported.

As well as the well nanotube dispersion, the strong interfacial adhesion between nanotubes and polymeric matrices is also a key factor for high-quality composites. Modifications of the CNT surface properties via covalent or noncovalent methods are considered as effective ways to improve dispersions of CNTs in polymer matrices and enhance interfacial adhesion [24–30]. Among them, the ideal approach [31–35] is to functionalize CNT surfaces with the matrix polymer for achieving an interfacial layer that is compatible with the matrix.

Here, we prepared polystyrene (PS)–MWCNT composites by melt-mixing on a kilogram scale using industrial large-scale polymer manufacturing machines like twin-screw extruder and injection moulding machine. The MWCNTs were well dispersed in the matrix and strong interfacial adhesion was achieved due to a PS layer, coating the nanotube surfaces through precipitation polymerization. The mechanical property of the composites was improved when incorporated with MWCNTs.

2. Experimental

2.1. Materials

The MWCNTs were prepared by catalytic decomposition of acetylene using catalyst of Ni/Mo/MgO [36] and then purified by chlorine oxidation [37]. Styrene was purchased from Beijing Chemical Plant and distilled before using. 2,2′-azobisisobutyronitrile (AIBN) was purchased from Alfa and used as received, and ethanol and tetrahydrofuran (THF) from Shanghai Chemical Plant. Industrial PS (Polystyrol 158 K) was obtained from Yangzi-BASF-Styrenics Co., Ltd.

2.2. Characterizations

Morphology observation was performed on a JSM-6700F scanning electron microscope (SEM, JEOL, Japan) at 15 kV. Transmission electronic microscope (TEM) observations of the purified MWCNTs and the modified MWCNTs (m-MWCNTs) were conducted on a TEM-3010 electron microscope (JEOL, Japan) at an acceleration voltage of 300 kV. TEM observations of the thin sections of PS–MWCNT composite were conducted on an H-800 electron microscope (Hitachi, Japan) at an acceleration voltage of 175 kV. Thin sections (with thickness of approximately 80 nm) were cut from the as-prepared PS–MWCNT composite under cryogenic conditions using an ultramicrotome (Leica, Austria) with a diamond knife. Izod impact test was performed with an XJ-40A pendulum apparatus (Wuzhong Materials Tester Factory, China) according to ASTMD 256. Tensile test was performed on a 4302 testing machine (Instron, UK) according to ASTMD 638.

2.3. Modification of MWCNTs

20.0 g purified MWCNTs, 20.0 ml distilled styrene, 0.1 g AIBN, and 600 ml ethanol were put into a three-necked flask and dispersed by KQ-5200DB ultrasonic instrument (40 kHz, Kunshan Ultrasonic Instruments Co., Ltd., China) for 30 min, maintaining the temperature below 30 °C. The flask was then transferred into a refitted MM823ESJ-PA microwave oven (Midea, China) and the mixture was irradiated (440 W) under nitrogen atmosphere, maintaining the refluxing of ethanol for 30 min. After cooling to room temperature, the mixture was filtrated through 0.2 μm pore-size polycarbonate membrane and the filtration residue was dried in vacuum at 100 °C for 24 h to achieve 25.0 g m-MWCNTs. About 15.0 g styrene was lost through forming oligomers that dissolved in ethanol and permeated through the membrane.

2.4. Masterbatch preparation of PS–MWCNT composite

20.0 g m-MWCNTs, 60.0 g PS, and 300 ml THF were put into a three-necked flask and stirred until the PS particles were completely dissolved. The mixture was dispersed by ultrasonication for 30 min, and then put into a 1000 ml beaker containing 600 ml ethanol with constant stir. Thus the masterbatch particles of PS–MWCNT composite were precipitated and then separated from the solvents by filtration. After drying in vacuum at 100 °C for 24 h, 79.8 g black masterbatch (m-masterbatch) was achieved. On the other hand, 16.0 g purified MWCNTs was directly mixed with 60.0 g PS through the same method to get 75.9 g masterbatch (p-masterbatch).

2.5. Preparation of PS–MWCNT composites

PS–MWCNT composites were prepared by melt-mixing of masterbatch and pure PS. For example, 16.0 g m-masterbatch and 3984.0 g pure PS were mixed in an SHR-10A high-speed-mixer (Zhangjiagangshi Zhenxiong Plastic Machinery, China) and then extruded with a TE-35 co-rotating twin-screw extruder (Coperion (Nanjing) Machinery Co., Ltd., China), which was equipped with a screw of 35.6 mm in diameter and L/D ratio of 38. The barrel temperature, from the entrance to the exit, was 190, 195, 200, 200, 190 and 185 °C, respectively. The melt of masterbatch and pure PS was blended for approximately 2 min through the shearing action of the rotating screws, which was held at a constant speed of 150 rpm. About 4.0 kg composite (PS–m-MWCNT composite) with 0.08 wt% MWCNT content was then achieved. Altering the ratio of the masterbatch to pure PS, we prepared extrudates of PS–m-MWCNT composite on a kilogram scale with varied nanotube contents such as 0.08 wt%, 0.16 wt%, 0.24 wt%, and 0.32 wt%. At the same time, p-masterbatch and PS were mixed by the same process to produce composite (PS–p-MWCNT composite) with varied nanotube contents (e.g. 0.08 wt%, 0.16 wt%, 0.24 wt%, and 0.32 wt%). The specimens for mechanical property test were molded using an HD-1300 injection machine (Hangzhou Huada Plastics Machinery Co., Ltd., China) with a screw of 45.0 mm in diameter, and L/D ratio of 20. The barrel temperature, from the entrance to the nozzle, was 190, 195, 200 and 190 °C, respectively.

3. Results and discussion

Fig. 1a–e shows TEM images of purified MWCNTs and m-MWCNTs. At low magnification, the purified MWCNTs (Fig. 1a) are clearer as compared with the blurry m-MWCNTs (Fig. 1b). This difference is probably due to a PS layer, wrapping the m-MWCNTs. In the high resolution (HR) TEM image of purified MWCNTs (Fig. 1c), the nanotube outer walls are lubricious due to the elimination of amorphous carbon, accordant to the early report [37]. On the contrary, there is a PS layer (called ‘PS coat layer’ in the following) on the surfaces of m-MWCNTs, as shown in Fig. 1d and e, so that the nanotubes can be separated from each other. Thereby,

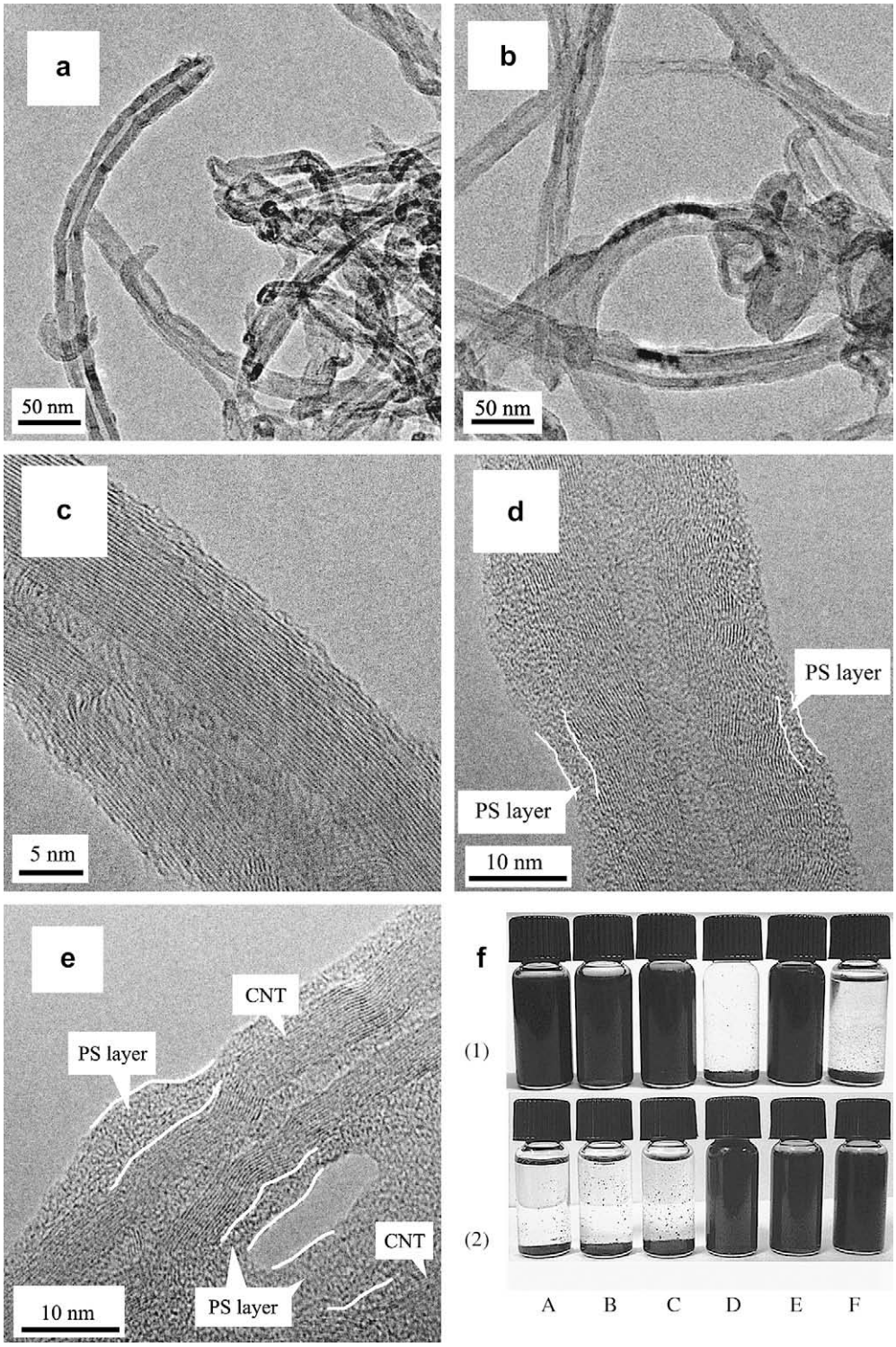

Fig. 1. TEM images of purified MWCNTs (a, c) and m-MWCNTs (b, d, and e); Dispersions of the purified MWCNTs (f(1)) and m-MWCNTs (f(2)) in (A) water, (B) ethanol, (C) acetone, (D) THF, (E) DMF, and (F) toluene, respectively, tranquilized for 7 days. For comparison, the concentration of all samples was 0.5 mg/ml.

with the assistance of the PS coat layer, the dispersion ability of nanotubes in PS matrix should be improved greatly.

To compare the dispersion ability of purified MWCNTs and m-MWCNTs, they were separately dispersed in water or organic solvents by ultrasonication for 30 min, tranquilized at room temperature, and then estimated with optical microscopy. The examined result of 7 days' tranquilization is shown in Fig. 1f. As detailedly demonstrated in the article [37], because of a large number of carboxyl groups and hydroxyl groups formed on the MWCNT surfaces during purification, the purified MWCNTs can be easily dispersed in polar solvents such as water, ethanol, acetone, and *N*,*N*-dimethylformamide (DMF), but they are precipitated from tetrahydrofuran (THF) and toluene. In this study, the same result was observed as shown in Fig. 1f(1), due to a same purification

utilized. However, the m-MWCNTs, coated by an apolar PS layer, are incompatible with polar solvents such as water, ethanol and acetone, proved by precipitations in Fig. 1f(2). On the other hand, because of the soluble PS layer, the stable dispersions of m-MWCNTs in THF, toluene, and DMF are separately observed in Fig. 1f(2). The dispersion varieties of purified MWCNTs and m-MWCNTs in tested solvents directly confirmed that the surface property of nanotubes was greatly altered by the PS coat layer.

In order to study the state of nanotubes, masterbatch was melted on a glass flake, then rapidly refrigerated to room temperature, introducing some cracks on the surface of masterbatch flake. Through the cracks, we can observe the nanotubes. Fig. 2a shows the typical resolution SEM image of p-masterbatch flake with a crack, in which the two matrix parts alongside the crack are separated from each other. At high magnification, one can clearly see in Fig. 2b that the nanotubes in the crack of p-masterbatch are unordered. Contrary to p-masterbatch flake, the two matrix parts alongside the crack in m-masterbatch flake are connected by nanotubes, shown in Fig. 2c. The nanotube axial directions (the white arrows in Fig. 2c) are all oriented and perpendicular to the extension directions of cracks (the black arrows in Fig. 2c), which are more clearly shown in Fig. 2d, the high resolution SEM image of m-masterbatch flake. The oriented nanotubes in cracks are attributed to the inducing stress caused by asymmetric volume shrinkage of PS matrix during rapid refrigeration, whose direction is also perpendicular to the extension direction of cracks. In addition, a nanotube network fabricated via weaving the oriented nanotubes with PS nanothreads is found in the crack of Fig. 2d. This network can efficiently connect the two matrix parts alongside the crack, avoiding the further extending of crack. These phenomena further prove that the PS coat layer plays a key role in improving the compatibility of nanotubes with PS matrix. One can clearly see that the average diameter of nanotubes in m-masterbatch (approximately 60 nm in Fig. 2d) is augmented in comparison to m-MWCNTs (approximately 40 nm in Fig. 2e), indicating the increase of the PS coat layer. Therefore, the nanotubes are further separated from each other and the homogeneous dispersion of nanotubes in m-masterbatch is expected, which has been confirmed by the individual oriented nanotubes in Fig. 2d.

As is known, the homogeneous dispersion of nanotubes in polymer matrices is one of the key factors for making high-performance composites, which was investigated by SEM and TEM in this study. As described in Fig. 3f, the fracture surface of the PS–MWCNT composite was perpendicular to the injection direction. Fig. 3a and c is the typical SEM images of the fracture surfaces of PS–p-MWCNT and PS–m-MWCNT composites, respectively. On the fracture surface of PS–p-MWCNT composite, there are many cavities formed by removing of nanotubes, indicating the poor polymer–nanotube interfacial adhesion. But on that of PS–m-MWCNT composite, there are many bright dots attributed to broken nanotube tips. This indicates that most of the nanotubes are broken rather than being pulled out in PS–m-MWCNT composite, suggesting a strong polymer–nanotube interfacial adhesion. The uniform distribution of the cavities and dots on the fracture surfaces shows that the nanotubes are homogeneously dispersed in the plane perpendicular to the injection direction. For further studying the state of nanotubes, the high resolution SEM was utilized to examine the images of the fracture surfaces of PS–p-MWCNT and PS–m-MWCNT composites, shown in Fig. 3b and d, respectively. In Fig. 3b, the broken nanotube tips in the fracture surface are completely disengaged from PS matrix, due to the poor interfacial adhesion. But in Fig. 3d, the broken nanotube tips are strongly bonded with PS matrix. An important phenomenon is the nanotubes pulled out the matrix are enwrapped by a bright middle layer of PS (see the black arrows in Fig. 3d) approximately 80 nm thickness at the bottoms, which is clearer in the magnified part of Fig. 3d. The bright middle layer can be evidently distinguished from the dark PS matrix. Moreover, the diameter of the nanotubes (see the white arrows in Fig. 3d) among PS middle layers is 80–130 nm, bigger than that (60 nm) of the nanotubes with a PS coat layer in Fig. 2d, due to a thicker PS coat layer. This indicates that the PS coat layer on the nanotube surfaces was further increased during melt-mixing. This difference between the PS coat layer and the PS middle layer is caused by different conjoinings with nanotubes, chemical bonds for the former and physical adsorptions for the latter. It was found that CNTs are excellent nucleating agents to enhance the crystallization rate of polymer matrix [38,39]. The middle layer is probably composed of the regular arrangement of PS chains near

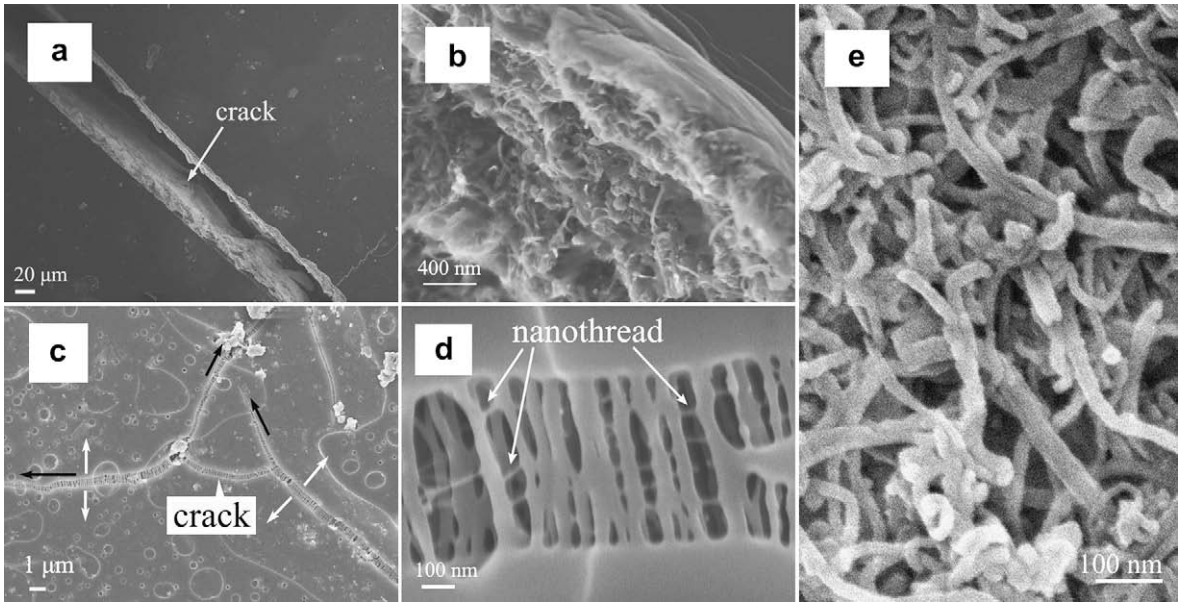

Fig. 2. SEM images of the p-masterbatch (a), m-masterbatch (c) and m-MWCNTs (e). (b) and (d) refer to the magnified images of cracks in (a) and (c), respectively.

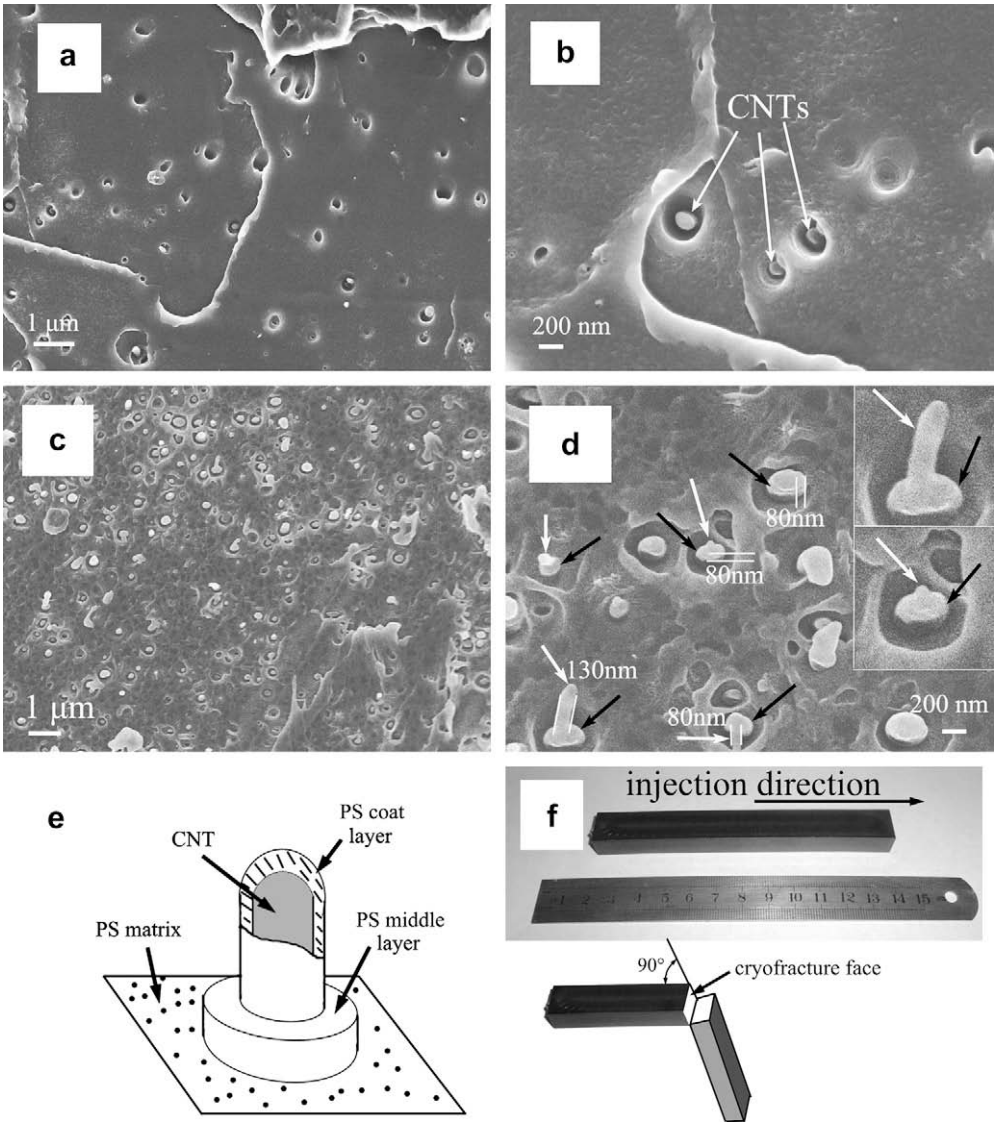

Fig. 3. SEM images of the cryofracture faces of PS–p-MWCNT (a,b) and PS–m-MWCNT (c,d) composites with 0.32 wt% nanotube content; Image of the broken nanotube tip on the cryofracture face of PS–m-MWCNT (e); Illustration (f) that the cryofracture face for SEM is perpendicular to the injection direction of the sample.

the nanotube surfaces, due to the nanotube inducing actions, whose mechanism study is currently underway in our group. Thereby, these bright dots, whose diameter is 200–400 nm, are the ends of broken nanotubes with a thick PS coat layer and a PS middle layer, whose morphology is illustrated in Fig. 3e. Despite the nanotubes are disengaged from the PS matrix, the middle layer strongly enwraps them like a coat, which indicates the strong interaction between the nanotubes and the middle layer. Additionally, there is a concave region around every bright dot, caused by the deformation of the matrix for the concentration of stress on the nanotubes, confirming the efficient stress transfer from the matrix to the nanotubes. These different nanotube states in PS–p-MWCNT and PS–m-MWCNT composites are resulted from the PS coat layer, which improved the compatibility between nanotubes and PS matrix, so that the middle layer was formed and the interfacial adhesion was enhanced.

TEM observation of a thin section is a common means utilized to investigate the nanotube dispersion in polymer matrices. As illustrated in Fig. 4a, the cutting direction of preparing thin sections is parallel to the injection direction of producing specimens (0.32 wt% CNT content). Through the thin sections, the nanotube state in the plane that parallels to the injection direction is observed, whose results are shown in Fig. 4b–f, where the nanotubes are individually dispersed in both PS–p-MWCNT and PS–m-MWCNT composites. Previous studies [17,40,41] reported that nanotubes could align by flow induced orientation in polymer–CNT composites. With respect to the disorganized axial directions of nanotubes in PS–p-MWCNT composite (the white arrows in Fig. 4b and c), the nanotubes in PS–m-MWCNT are extended and oriented to one direction (the white arrows in Fig. 4d–f) that is identical with the direction of scraping traces (the black arrows in Fig. 4a–f) caused by the cutting of making thin sections. Thereby, it can be suggested that the nanotubes are oriented along the injection direction under the shearing forces during injection process of PS–m-MWCNT composite, which further proves that the dispersion ability of nanotubes in PS matrix was strongly improved by the PS layers (coat layer and middle layer). On the basis of these results, it can be considered that the individual nanotube dispersion in polymer matrix is possible via melt-mixing using industrial large-scale manufacturing machines.

Tensile test and Izod impact test were performed to evaluate the effect of the MWCNTs on the mechanical properties of PS–MWCNT composites, whose results are shown in Fig. 5, where the addition of

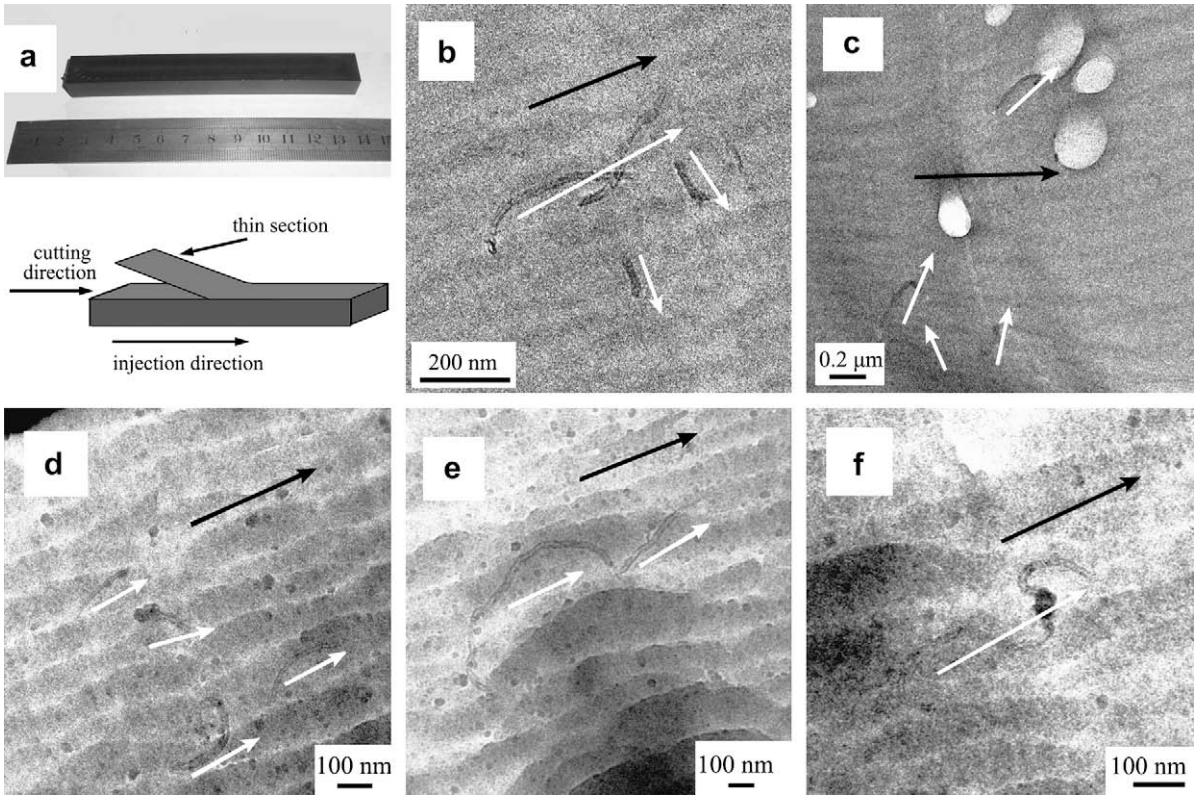

Fig. 4. Illustration (a) that the thin section for TEM is parallel to the injection direction of the cubical sample; TEM images of the thin sections of PS–p-MWCNT (b,c) and PS–m-MWCNT (d,e, and f) composites with 0.32 wt% nanotube content. The black arrows in (b)–(f) refer to the directions of scraping traces, and the white arrows refer to the nanotube orientations.

MWCNTs improved the impact strength (Fig. 5a). When the MWCNT content is 0.32 wt%, the impact strength of PS–m-MWCNT composite is 3.74 kJ/m^2, significantly increased by 250% in comparison to that of pure PS, while the impact strength of PS–m-MWCNT composite is only 2.24 kJ/m^2 (increased 150%). In the case of PS–m-MWCNT composite, the nanotubes are extended and oriented along the injection direction that is just perpendicular to the impact stress during Izod impact test. Because of the high length–diameter ratio of nanotubes and the strong interfacial adhesion, the m-MWCNTs can share in a large amount of impact energy through the deformation of themselves, inducing the significant increase of impact strength. Contrarily, the lack of oriented nanotubes and the poor interfacial adhesion in PS–p-MWCNT composite result in a lower increase of impact strength. In Fig. 5b, the tensile strength of PS–p-MWCNT and PS–m-MWCNT composites is slightly varied with the increase of nanotube content. Because of the low content and the individual nanotubes (shown in Fig. 4b–f), a nanotube network for reinforcing the composite cannot be formed, which results in the slight change of tensile strength. In PS–p-MWCNT composite, the stress cannot be efficiently transferred to nanotubes from matrix due to the poor interfacial adhesion, leading to the slight decrease of tensile strength. Contrarily, the strong interfacial adhesion and efficient stress transfer in PS–m-MWCNT composite result in the slight increase of tensile strength.

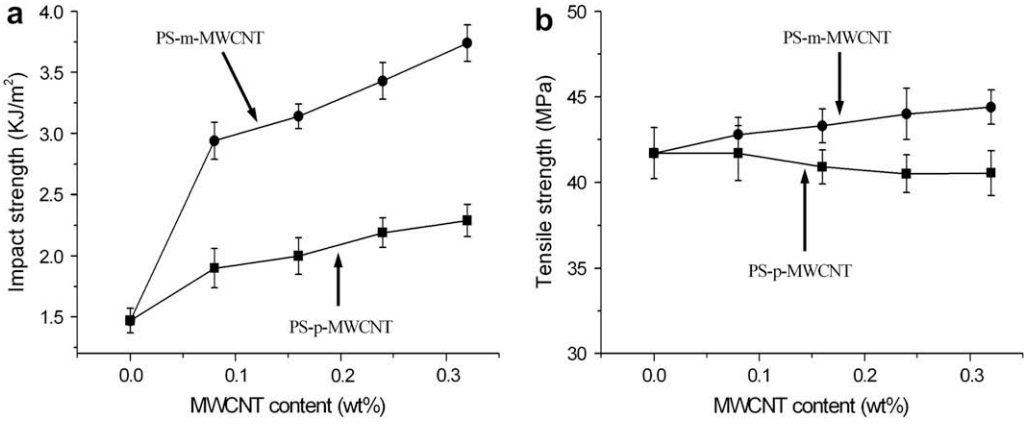

Fig. 5. Effect of MWCNT content in PS–MWCNT composites on the impact strength (a) and tensile strength (b).

4. Conclusions

In summary, the dispersion ability of nanotubes was greatly improved by a PS coat layer. Microscopic investigation of the PS–MWCNT composites indicated that there was a PS middle layer between the m-MWCNTs and PS matrix; whereas, this layer was inexistent in PS–p-MWCNT composite. Due to the PS coat layer and PS middle layer, the compatibility of nanotubes and PS matrix was greatly enhanced, leading to a strong interfacial adhesion and nanotube orientation. Thereby, as compared to the pure PS, the PS–m-MWCNT composite showed a higher increase of impact strength than the PS–p-MWCNT composite. Additionally, the tensile strength of PS–m-MWCNT composite was slightly ascending with the addition of nanotube content; whereas, that of PS–p-MWCNT composite was slightly descending. Thus it can be seen that both the homogeneous dispersion of nanotubes and the strong interfacial adhesion are comparably important for an excellent polymer–nanotube composite.

Acknowledgments

This work was supported by National Nature Science Foundation of China (No. 50772033) and SIT projects of Hunan University. The authors thank Dr. Zhu Jintao (Polymer Science and Engineering at the University of Massachusetts Amherst) for his good advice.

References

[1] Hsiao C-C, Lin TS, Cheng LY, Ma C-CM, Yang AC-M. Macromolecules 2005;38:4811–8.
[2] Sen R, Zhao B, Perea D, Itkis ME, Hu H, Love J, et al. Nano Lett 2004;4:459–64.
[3] Yu J, Lu K, Sourty E, Grossiord N, Koning CE, Loos J. Carbon 2007;45:2897–903.
[4] Ruan S, Gao P, Yu TX. Polymer 2006;47:1604–11.
[5] Safadi B, Andrews R, Grulke EA. J Appl Polym Sci 2002;84:2660–9.
[6] Chang T-E, Kisliuk A, Rhodes SM, Brittain WJ, Sokolov AP. Polymer 2006;47:7740–6.
[7] Jia ZJ, Wang ZY, Xu CL, Liang J, Wei BQ, Wu DH, et al. Mater Sci Eng A 1999;271:395–400.
[8] Park C, Ounaies Z, Watson KA, Crooks RE, Smith JJ, Lowther SE, et al. Chem Phys Lett 2002;364:303–8.
[9] Pötschke P, Bhattacharyya AR, Janke A. Carbon 2004;42:965–9.
[10] Andrews R, Jacques D, Minot M, Rantell T. Macromol Mater Eng 2002;287:395–403.
[11] Biercuk MJ, Llaguno MC, Radosavljevic M, Hyun JK, Johnson AT, Fischer JE. Appl Phys Lett 2002;80:2767–9.
[12] McNally T, Pötschke P, Halley P, Murphy M, Martin D, Bell SEJ, et al. Polymer 2005;46:8222–32.
[13] Kanagaraj S, Varanda FR, Zhil'tsova TV, Oliveira MSA, Simões JAO. Compos Sci Technol 2007;67:3071–7.
[14] Grossiord N, Miltner HE, Loos J, Meuldijk J, Mele BV, Koning CE. Chem Mater 2007;19:3787–92.
[15] Pegel S, Pötschke P, Petzold G, Alig I, Dudkin SM, Lellinger D. Polymer 2008;49:974–84.
[16] Pötschke P, Fornes TD, Paul DR. Polymer 2002;43:3247–55.
[17] Haggenmueller R, Gommans HH, Rinzler AG, Fischer JE, Winey KI. Chem Phys Lett 2000;330:219–25.
[18] Jin JX, Pramoda KP, Xu GQ, Goh SH. Chem Phys Lett 2001;337:43–7.
[19] Lozano K, Barrera EV. J Appl Polym Sci 2001;79:125–33.
[20] Lozano K, Bonilla-Rios J, Barrera EV. J Appl Polym Sci 2001;80:1162–72.
[21] Zou YB, Feng YC, Wang L, Liu XB. Carbon 2004;42:271–7.
[22] Chen L, Pang XJ, Yu ZL. Mater Sci Eng A 2007;457:287–91.
[23] Villmow T, Pötschke P, Pegel S, Häussler L, Kretzschmar B. Polymer 2008;49:3500–9.
[24] Kuan C-F, Kuan H-C, Ma C-CM, Chen C-H, Wu H-L. Mater Lett 2007;61:2744–8.
[25] Star A, Stoddart JF. Macromolecules 2002;35:7516–20.
[26] Vaisman L, Marom G, Wagner HD. Adv Funct Mater 2006;16:357–63.
[27] Sahoo NG, Jung YC, Yoo HJ, Cho JW. Macromol Chem Phys 2006;207:1773–80.
[28] Niyogi S, Hu H, Hamon MA, Bhowmik P, Zhao B, Rozenzhak SM, et al. J Am Chem Soc 2001;123:733–4.
[29] Sun Y-P, Huang W, Lin Y, Fu K, Kitaygorodskiy A, Riddle LA, et al. Chem Mater 2001;13:2864–9.
[30] Huang W, Lin Y, Taylor S, Gaillard J, Rao AM, Sun Y-P. Nano Lett 2002;2:231–4.
[31] Qin S, Qin D, Ford WT, Resasco DE, Herrera JE. Macromolecules 2004;37:752–7.
[32] Lin Y, Zhou B, Fernando KAS, Liu P, Allard LF, Sun Y-P. Macromolecules 2003;36:7199–204.
[33] Blond D, Barron V, Ruether M, Ryan KP, Nicolosi V, Blau WJ, et al. Adv Funct Mater 2006;16:1608–14.
[34] Li H, Cheng F, Duft AM, Adronov A. J Am Chem Soc 2005;127:14518–24.
[35] Yang B-X, Pramoda KP, Xu GQ, Goh SH. Adv Funct Mater 2007;17:2062–9.
[36] Li Y, Zhang XB, Tao XY, Xu JM, Huang WZ, Luo JH, et al. Carbon 2005;43:295–301.
[37] Yuan J-M, Chen X-H, Chen X-H, Fan Z-F, Yang X-G, Chen Z-H. Carbon 2008;46:1266–9.
[38] Wang C, Huang CL, Chen YC, Hwang GL, Tsai SJ. Polymer 2008;49:5564–74.
[39] Gao Y, Wang Y, Shi J, Bai H, Song B. Polym Test 2008;27:179–88.
[40] Cipriano BH, Kota AK, Gershon AL, Laskowski CJ, Kashiwagi T, Bruck HA, et al. Polymer 2008;49:4846–51.
[41] Fornes TD, Baur JW, Sabba Y, Thomas EL. Polymer 2006;47:1704–14.